Improvement of Gene Delivery and Mutation Efficiency in the CRISPR-Cas9 Wheat (*Triticum aestivum* L.) Genomics System via Biolistics

Jaclyn Tanaka[1], Bastian Minkenberg[1,*], Snigdha Poddar[1,2], Brian Staskawicz[1,3], Myeong-Je Cho[1,✉]

Abstract

Discovery of the CRISPR-Cas9 gene editing system revolutionized the field of plant genomics. Despite advantages in ease of designing gRNA and the low cost of the CRISPR-Cas9 system, there are still hurdles to overcome in low mutation efficiencies, specifically in hexaploid wheat. In conjunction with gene delivery and transformation frequency, the mutation rate bottleneck has the potential to slow down advancements in genomic editing of wheat. In this study, nine bombardment parameter combinations using three gold particle sizes and three rupture disk pressures were tested to establish optimal stable transformation frequencies in wheat. Utilizing the best transformation protocol and a knockout cassette of the phytoene desaturase gene, we subjected transformed embryos to four temperature treatments and compared mutation efficiencies. The use of 0.6 µm gold particles for bombardment increased transformation frequencies across all delivery pressures. A heat treatment of 34°C for 24 hours resulted in the highest mutation efficiency with no or minimal reduction in transformation frequency. The 34°C treatment produced two M_0 mutant events with albino phenotypes, requiring biallelic mutations in all three genomes of hexaploid wheat. Utilizing optimal transformation and heat treatment parameters greatly increases mutation efficiency and can help advance research efforts in wheat genomics.

(1) Innovative Genomics Institute, University of California, Berkeley, CA, USA,
(2) Department of Molecular and Cell Biology, University of California, Berkeley, CA, USA,
(3) Department of Plant and Microbial Biology, University of California, Berkeley, CA, USA
*Present address: Inari Agriculture, Inc., Cambridge, MA, USA

✉ Corresponding author: e-mail: mjcho1223@berkeley.edu

Keywords: wheat, transformation, biolistics, microparticle size, rupture disk pressure, high temperature, genome editing, phytoene desaturase gene (PDS), albino phenotype

Introduction

Wheat is grown on more land than any other crop and is the second most produced grain in the world behind maize. It serves as a staple food worldwide, accounting for a fifth of globally consumed calories (http://www.fao.org/faostat/en). It is an important source of carbohydrates and is the leading source of vegetable-based protein in the human diet. World trade for wheat is greater than all other grains combined, which in effect has a great impact on global food security. With looming changes to the environment brought on by climate change as well as a growing global population, the need to address issues such as drought, yield and disease in wheat is critical. Our ability to edit wheat to produce more robust plants that can take on changing environmental landscapes and societal needs is imperative.

Bread wheat is genetically hexaploid (Hart 1983) which makes breeding more complicated than other cereals such as rice and maize as a result of the triple genomes. Traditionally, wheat has been bred by crossing two lines by hand and subsequently segregating progeny for the desired traits. This task is time consuming and takes multiple generations to achieve the necessary genetic composition due to the hexaploid nature of wheat. It can take years for a wheat cultivar to be established for commercial use through traditional breeding.

More modern development of wheat varieties is obtained through indirect or direct gene transfer, typically via *Agrobacterium* and particle bombardment, respectively. Through *Agrobacterium*-mediated transformation, selected genes are transferred from bacteria to plant cells via disarmed *Agrobacterium* vectors (Smith and Hood 1995) and whole plants are then generated through tissue culture. *Agrobacterium*-mediated transformation has been well established in a variety of crops and is advantageous for intact transfer of larger DNA fragments (Dai et al. 2001). Although *Agrobacterium*-mediated transformation can result in high instances of single-copy events and intact T-DNA delivery, it lacks consistency across species, genotypes and tissue types especially in more recalcitrant varieties (Smith and Hood 1995; Hu et al. 2003). This specificity limits the ability for impact across multiple crops or cultivars in addition to more regulatory hurdles involved with the transfer of *Agrobacterium* binary backbone.

Conversely, particle bombardment is a method of direct gene transfer in which DNA is precipitated onto gold particles and delivered onto plant tissue using high pressure Helium gas (Klein et al. 1988; Vain et al. 1993; Lemaux et al. 1996; Finer et al. 2000). In this system there are multiple factors that can be adjusted to optimize DNA delivery such as the size of gold particles, amount of gold particles, delivery pressure, amount of DNA and distance from the plant tissue. We chose to use particle bombardment as our gene delivery system because it is less species-

and genotype-dependent and vector construction is simpler. Although particle bombardment can have higher instances of multiple copy events, the copies are often located on the same locus allowing for easy segregation out in future generations. Choi et al. (2002) showed that 18 out of 19 independent transgenic barley events generated via bombardment had transgene integration at a single locus. In addition, since particle bombardment is a form of direct gene delivery it is a mechanism that is unregulated and can result in a more streamlined regulatory process.

In the forefront of genetic engineering today is gene editing and CRISPR (Doudna and Charpentier 2014). The CRISPR-Cas9 gene editing system is widely used for improvement of various field crops (Bortesi and Fischer 2015). The system allows researchers to utilize short repeats of endogenous DNA in the plant genome derived from bacteriophages to identify specific locations in the genome for gene editing. In conjunction with these DNA repeats, the Cas9 protein is programmed to cut double-stranded DNA in precise locations and allows for site-specific editing within the plant genome. The ability to make site-specific gene edits in a plant gives this technology an advantage over traditional genetic modification methods that randomly insert DNA. The CRISPR-Cas9 system allows for not only the insertion of new DNA into the plants but also the deletion or silencing of single genes within the genome that can confer a variety of advantageous phenotypes.

Mutation efficiencies using the CRISPR-Cas9 system vary widely across monocot species. Rice mutation efficiencies are generally higher compared to wheat mutation efficiencies (Feng et al. 2013; Howells et al. 2018; Liu et al. 2019; Zhang et al. 2019). In addition, mutation efficiencies are largely impacted by the individual components of a construct. The proper selection of promoters to drive expression of Cas9 and sgRNAs can increase expression levels and ultimately positively impact mutation efficiency in transformed plants. In addition, testing sgRNA sequence efficiency *in vivo* before stable transformation is critical for maximizing mutation efficiency (Poddar et al. 2020). Even the sequence of Cas9 protein can affect mutation efficiency, through codon optimization and the presence or absence of introns (Grützner et al. 2021). At the plant level, mutation efficiency is dependent on establishing an effective tissue culture protocol which is predominantly reliant on identifying a good starting explant. Another approach to increase mutation efficiency in plants is the effect of temperature treatments. The effect of temperature treatments on mutation efficiencies has been proven in mammalian cell culture (Xiang et al. 2017). The CRISPR-Cas9 system was established on a principle derived from *Streptococcus pyogenes* adaptive immunity to viruses (Doudna and Charpentier 2014). *S. pyogenes* grows the most dynamically at 40°C (Panos and Cohen 1964). It is reasonable to expect that the Cas9 protein will be more efficient at higher temperatures. Recent studies have reported positive effects of

temperature treatment on editing efficiency in *Arabidopsis*, citrus, rice and wheat plants (LeBlanc et al. 2018; Malzahn et al. 2019; Milner et al. 2020).

The phytoene desaturase gene (PDS) is commonly applied as a demonstration of experimental mutation efficiencies due to its visual phenotype and wide conservation across species. The PDS gene is involved in the carotenoid synthesis pathway (Bartley and Scolnik 1995) in plants. A recessive mutation, or knockout, of the PDS gene disrupts the formation of β-carotene and confers a visual albino phenotype (Qin et al. 2007). The PDS knockout has been demonstrated in a range of species including, but not limited to, *Arabidopsis* (Qin et al. 2007), rice (Zhang et al. 2014), banana (Naim et al. 2018), cassava (Odipio et al. 2017) and melon (Hooghvorst et al. 2019). However, the PDS knockout, albino phenotype, has not been previously reported in M_0 hexaploid wheat because it is likely to require biallelic mutations on all six loci of the three genomes.

Finding a good combination of these factors to increase CRISPR mutation efficiency in wheat is a valuable tool for facilitating the production of robust wheat cultivars that can withstand the effects of climate change faster than other approaches. In this study, we establish parameters for particle bombardment that result in improved transformation frequencies, as well as subsequent temperature treatments to increase mutation efficiencies in hexaploid wheat. We also report the successful generation of PDS triple recessive mutant events in the M_0 generation displaying the albino phenotype. In addition, we demonstrate the albino phenotype in M_1 and M_2 progeny plants derived from an edited event with monoallelic and biallelic mutations in the 3 different genomes.

Materials and Methods

Plant Material

Seeds of *Triticum aestivum* L. cv. Fielder were sown weekly and grown in growth chambers under 16-hr days at 24°C, and 8-hr nights at 15°C. Light levels were set to approximately 130 µmol m^{-2} s^{-1} at head height. Immature spikes were harvested 10-14 days post flowering with an immature embryo (IE) sized 1.7-2.2 mm. Immature spikes were collected up to 5 days pre bombardment and stored at 4-6°C. One day prior to bombardment, immature seeds were harvested from immature spikes and surface-sterilized using 20% (v/v) bleach (8.25% sodium hypochlorite) plus one drop of Tween 20 for 15 minutes before triple rinsing with sterile water. IEs were then isolated and placed scutellum side up on DBC3 medium (Cho et al. 1998) and incubated at 26°C overnight.

137

138 ***Plasmids***

139 Plasmids, pAct1IHPT-4, pAct1IDsRED and pRGE610-PDS-PS2, were used for transformation
140 (Fig. 1). pAct1IHPT-4 (Cho et al. 1998) and pAct1IDsRED contain hygromycin
141 phosphotransferase (*hpt*) and *DsRED* genes, respectively, each under control of the rice actin 1
142 promoters, its intron (*act1I*) and the nos 3' terminator (Figs. 1A and B). pRGE610-PDS-PS2
143 contains Cas9 gene and gRNA cassettes (Fig. 1C) and was made using the following steps. First,
144 the wheat U6 promoter with blue-white screening cassette was amplified from pTaU6-sgRNA (gift
145 from Daniel Voytas) with primers TaU6Lac-*Hin*dIII-F (5'-
146 TAAAGGAACCAATTCAGTCGACTGGAT-3') and TaU6Lac-*Sbf*I-R (5'-
147 GCCCTGCAGGTCTAGATATCTCGAGGGTACCAAACTGAG-3'). pRGE32 (gift from Yinong
148 Yang, Addgene ID 63159) was digested with *Sbf*I and *Hin*dIII to release the original sgRNA
149 cassette. Then, the PCR fragment from the first step was ligated into the digested pRGE32
150 backbone to create pRGE610. Next, two fragments from pGTR (gift from Yinong Yang, Addgene
151 ID 63143) were amplified. The first fragment, product of TaU6-L5AD-*Btg*ZI-F (5'-
152 CGGGTCTCACTTGGCGATGTCTTGGTCTGCTTGACAAAGCACCAGTGG-3') and PDS-PS2-
153 gR (5'-TAGGTCTCAAGGTGGTCATTGCACCAGCCGGG-3'), contained a tRNA and the first half
154 of the sgRNA spacer PS2 with 4 bp overhangs on each site to enable Golden Gate assembly with
155 the second fragment. The second fragment, product of PDS-PS2-gF (5'-
156 CGGGTCTCCACCTTCTTTTCAGCGTTTTAGAGCTAGAA-3') and L3AD-*Btg*ZI-R (5'-
157 TAGGTCTCCAAACGCGATGGAGCGACAGCAAACAAAAAAAAAAGCACCGACTCG-3'),
158 contained the second half of PS2 followed by the sgRNA scaffold and overhangs for Golden Gate
159 assembly on each site. The NEB® Golden Gate Assembly Kit (BsaI-HF®v2) was used to combine
160 both fragments. The resulting product was used as template for primers TaU6-S5AD-*Btg*ZI-F (5'-
161 CGGGTCTCACTTGGCGATGTCTTGGTCTGCTTG-3') and S3AD-*Btg*ZI-R (5'-
162 TAGGTCTCCAAACGCGATGGAGCGACAGCAAAC-3') to yield enough of the Golden Gate
163 assembly product for digestion with *Btg*ZI. The *Btg*ZI digested product was then ligated into the
164 *Bsa*I digested backbone of pRGE610, to finally create pRGE610-PDS-PS2.

165

166 ***Stable Transformation via Particle Bombardment***

167 Immature embryos, isolated from immature spikes (Fig. 2A) and pre-incubated at 26°C overnight,
168 were used for bombardment. On the day of bombardment, IEs were placed on top of a 40 mm
169 filter paper on a plate of DBC3 osmoticum medium containing mannitol and sorbitol (0.2 M each)
170 (Fig. 2B, Cho et al. 2000). Four hours after treatment with osmoticum, IEs were bombarded using

Bio-Rad PDS-1000/He particle gun (Fig. 2C) as previously described (Lemaux et al. 1996; Cho et al. 2000) with modifications. Two milligrams of gold particles (0.4, 0.6 and 1.0 µm) were coated with 5 µg of a mixture of pAct1IHPT4 and pAct1IDsRED or pAct1IHPT4 and pRGE610-PDS-PS2 at a 1:2 ratio. Each particle prep was resuspended in 85 µL of 100% EtOH and 7.5 µL was spread onto the center of a macrocarrier inside of a macrocarrier holder. The particle preps were used for bombardment with a Bio-Rad PDS-1000/He biolistic device (Bio-Rad, Hercules, CA) at 3 different delivery pressures (650, 900 and 1100 psi). Each plate of IEs was bombarded twice per treatment. After bombardment, IEs were transferred from filter paper to the exposed media and incubated overnight at 26°C in dim light (10-30 µmol m^{-2} s^{-1}). Sixteen hr post bombardment, IEs were transferred to DBC3 medium and incubated at 26°C for 1 wk in dim light. Following the resting period, IEs went through 3 rounds of selection via DBC3 media containing 30 mg/l hygromycin B, each round of selection lasting 3 wk (Fig. 2D). After the third round of selection, regeneration was initiated using DBC6 media (Cho et al. 2015) containing 30 mg/l hygromycin B and incubated at 26°C in high light (90 µmol m^{-2} s^{-1}) and subcultured every 3 wk. Once shoots were approximately 0.5-3.0 cm in height (Fig. 2E), shoots were transferred to WR rooting media for root formation. Plantlets were then transferred to soil once they had enough shoots to support transplant to soil (Fig. 2F).

Temperature Treatment of Bombarded Immature Embryos

Bombarded IEs were subjected to varying heat treatments of 26°C, 30°C, 34°C and 37°C 4 days post bombardment for 24 hr, incubated in Heratherm Compact Microbiological Incubators (Thermo Scientific, Cat# 50125590, Grand Island, NY).

Non-bombarded IEs with temperature treatments were tested for tissue culture response. The IEs were isolated onto DBC3 medium and incubated for 1 day. The following day they were placed on DBC3 osmoticum medium for 20 hours to replicate the same treatment as bombarded IEs. The IEs were then transferred back to DBC3 medium for 3 days and then split up and treated with heat treatments of 26°C, 30°C, 34°C and 37°C for 24 hours. IEs were allowed to grow and proliferate into callus for 5 weeks at which point the callus in each plate was collectively weighed for comparison.

Fluorescent visualization

Fluorescent images of IEs, calli and plantlets of transgenic Fielder events were visualized with a fluorescent Leica M165 FC stereomicroscope, equipped with Leica DFC7000 T (JH Technologies, Fremont, CA), using two microscopic filters, brightfield and ET DSR with 545 nm excitation and

620 nm emission. The microscope is linked to a camera imaging software, Leica Application Suite version 4.9, which was used to capture the fluorescent images. Screening of fluorescent activity was measured at different magnifications.

Detection of Transgenes and CRISPR/Cas9 Mutations

Genomic DNA was extracted from leaf tissue following a CTAB extraction method (Murray and Thompson 1980). The *hpt, dsRED*, and *Cas9* transgenes were confirmed by PCR using sequence specific primers (Table S1). Amplifications were performed in a 25-µl reaction with DreamTaq PCR Master Mix (2X) (Thermo Fisher Scientific, Grand Island, NY) as described (Jones et al. 2022). For each PCR reaction, 23 µL were loaded onto a 0.8% agarose gel for electrophoresis.

For detection of PDS mutations, a fragment within range of the desired mutation was targeted via homoallele specific primers across each genome (Table S1) and amplified by PCR. The amplified PCR product was cut, and DNA was extracted from gel samples using the Qiagen QIAquick Gel Extraction Kit (QIAGEN, Chatsworth, CA). The purified DNA samples were used for Sanger sequencing. Mutation efficiency was calculated as the number of mutated unique events per treatment divided by the total number of events regenerated from the same treatment.

M1 Mutation screening

Mutation line PC14A containing monoallelic mutations in the A and D genomes and a heterozygous biallelic mutation in the B genome was chosen for next generation progeny screening. M_1 IEs sized 2.0-3.0 mm were harvested from the M_0 plant. IEs were surface sterilized with 20% bleach plus one drop of Tween 20 for 15 minutes. Sterilized IEs were triple rinsed with sterile water to remove excess bleach. IEs were then excised and placed on WR medium scutellum side down for germination. Once plantlets germinated, progeny were visually assessed for phenotype and sampled for genotyping and mutation analysis.

Results and Discussion

Optimization of Particle Bombardment Parameters for Plant Transformation

Gold Particle Size and Transformation Frequency

The DsRED visual marker was used to assess the particle bombardment parameters and stable transformation frequencies. Transient DsRED expression driven by the rice actin 1 promoter and

its intron was initially detected 1 day after particle bombardment of wheat (cv. Fielder) IEs and was clear 2 to 3 days post bombardment (Fig. 3A). DsRED-expressing sectors were formed (Fig. 3B), and stably transformed plantlets were generated 6-8 weeks and 10-12 weeks post bombardment, respectively (Figs. 3C and D).

Three gold particle sizes, 0.4 µm, 0.6 µm and 1.0 µm, were tested to compare their effects on transformation frequency. The size and weight of the individual particles has an effect on its ability to physically deliver DNA to the plant cell. It was observed that the 0.6 µm gold particles performed best in transformation frequency across all delivery pressures with an average frequency of 22.6% (Table 1). The 0.4 µm particles performed second best but with an average transformation frequency of 10.7% that measured well below that of 0.6 µm. However, the 1.0 µm particles resulted in the lowest average transformation frequency of 9.0%. In our study, we used the same weight of gold particles and the same amount of DNA per prep, meaning that the larger-sized particles will have fewer particles than the smaller-sized ones. Theoretically,1.0 µm particles have 4.5-fold and 16.7-fold less number of particles per weight than 0.6 µm and 0.4 µm particles, respectively, because gold particle volume (weight) is calculated as $(4/3)\pi r^3$ (r = radius) (Fig. 3A). Therefore, the use of 1.0 µm gold particles resulted in a lower transformation frequency likely due to a smaller number of particles per bombardment compared to 0.6 µm particles (Table 1). In addition, the large particles can damage the cells beyond their ability to recover and subsequently negatively affects regeneration of transgenic plants. However, our results from the 0.4 µm vs 0.6 µm comparison showed that transformation frequency (22.6%) with 0.6 µm particles was 2.1-fold higher than that (10.7%) with 0.4 µm particles (Table 1), even though the number of 0.6 µm particles were 3.7-fold less than that of 0.4 µm particles (Fig. 3). This is possibly due to the smaller amount of DNA coated onto 0.4 µm particles or reduced capability of 0.4 µm particles to penetrate the target cells of IEs, compared to 0.6 µm particles.

The theoretical calculation of the surface area of a sphere ($4\pi r^2$) shows us that gold particle size positively correlates to surface area (Fig 3B). As the diameter, or radius, of a gold particle increases so does the surface area of the sphere. This means that particle size alters the DNA-holding capacity of a single particle. From 0.4 µm to 1.0 µm diameters, the surface area increases by 6.25-fold. In our study, we used the same weight of gold particles and the same amount of DNA per prep, meaning theoretically the 1.0 µm gold particles can hold 6.25-fold more DNA than the 0.4 µm particles allowing for a higher percentage of DNA delivery upon impact with the plant cells. Our data supports this theory, indicating that co-expression efficiency increases as particle diameter increases. Co-expression efficiency is calculated as the number of events visually expressing dsRED over the total number of events generated using hygromycin selection.

The 1.0 µm particle size had the highest co-expression efficiency of 46.9%, 0.6 µm in the middle with 32.4% and 0.4 µm was the lowest with a co-expression efficiency of 14.3% (Table 2S). However, when optimizing transformation, 1.0 µm was not selected as a candidate due to its low transformation frequency regardless of its high DNA delivery performance.

Delivery Rupture Pressure and Transformation Efficiency

Different species and tissue types can require different rupture pressures to optimize transformation frequency. We tested three rupture pressures, 650 psi, 900 psi and 1100 psi for each of the three particle sizes (Table 1). For the 0.4 µm particle size, both the 650 psi and 900 psi resulted in higher transformation frequencies of 12.9% and 13.6%, respectively, compared to 1100 psi (7.7%). Rupture pressures of 650 psi, 900 psi and 1100 psi resulted in similar frequencies for the 0.6 µm particle size at 24.3%, 21.6% and 21.9%, respectively. The 1.0 µm particle size resulted in the lowest transformation frequencies of 7.9%, 9.0% and 10.3% for the 650 psi, 900 psi and 1100 psi rupture pressures. In analyzing this data, we found that a 650 psi rupture pressure was optimal for both the 0.4 µm and 0.6 µm particle sizes while 1100 psi was optimal for the 1.0 µm particle size. However, given the low transformation frequencies, 1.0 µm at any rupture pressure is not recommended.

Initially, we hypothesized that the smaller the particle size, the higher the rupture pressure would need to be to maximize delivery of the particles to the tissue. However, we found that even using the smallest particle size, 0.4 µm, at the lowest pressure of 650 psi was optimal. The 1.0 µm particle size is larger and heavier and performs better at 1100 psi leaving us to conclude that a higher pressure is required to deliver larger particles to the plant tissue, indicating that larger-sized gold particles may have more resistance for penetrating the plant cells

Optimization of Mutation Efficiency in PDS Gene-Edited Wheat

High Temperature Treatments and Mutation Efficiency

Although the Cas9 protein may be most active and efficient at 40°C, the plant cells cannot survive a prolonged exposure to such a high temperature (Panos and Cohen 1964). The key to finding the optimal temperature is one that satisfies both protein and plant. We initiated heat treatment tissue culture experiments testing callus growth of 10 Fielder embryos on standard DBC3 media after DBC3 osmoticum treatment with a temperature range of 26°C, 30°C, 34°C and 37°C for 1 day to monitor tissue morphology over time. To quantify the effect of heat treatment on the callus tissue, we weighed the tissue 35 days post isolation. Evaluation of the callus tissue weight from

each treatment allowed us to quantify the effects of heat treatment. Both the 30°C and 34°C heat treatments weighed similar to the control without heat treatments at 1.59 g and 1.70 g, respectively, while the control of 26°C weighed 1.66 g (Table 2). This demonstrated that plant cells are capable of long-term normal to accelerated growth after subjection to a slightly increased temperature for a short period of time. The 37°C plate, however, grew at a slower rate, weighing in at only 1.37 g. This indicates that higher temperatures even for short periods of time negatively affects tissue growth over time in addition to tissue quality. Negative effects on the tissue growth rate and tissue quality will impact transformation frequencies and thus mutation efficiencies of experiments.

We designed our PDS mutation efficiency experiment to confirm the effects of heat treatment on mutation efficiency in plants on a significant scale side by side with our dsRED + hpt transformation frequency experiment. We chose our bombardment parameters based on the data set with the most promising transient dsRED expression and transformation efficiency. We used 0.6 µm at 2 different rupture pressures, 650 psi and 1100 psi and tested a total of 4 temperature treatments 26°C, 30°C, 34°C and 37°C for 24 hours, 4 days post bombardment (Table 3). We expected to see higher mutation frequencies at higher temperatures because of previously reported increased Cas9 activity at higher temperatures consistent with previous studies testing 22°C, 28°C, 32°C and 37°C in rice protoplasts, maize plants and *Arabidopsis* (LeBlanc et al 2018; Malzahn et al. 2019). In the Mazahn study (2019), temperatures between 28°C and 32°C proved to increase the Cas9 activity *in vivo*. However, their mutation efficiencies were reported via production of M_1 mutants via heat treatment of M_0 maize plants containing Cas9 and gRNA; transgenic plantlets were not produced via transformation in rice. Similarly, in the LeBlanc study (2018), *Arabidopsis* and citrus plants were treated with four, 30-hr exposures to 37°C during the vegetative growth stage as opposed to the control of 22°C. In their experiment, loss of GFP expression in the transgenic plantlets conferred mutation. They reported an increase in mutation frequencies in comparison to their control as well, recording 12% GFP expression in plantlets treated with 37°C as compared to the control at 89% GFP expressing plantlets. Exposing transformed embryos to heat a heat treatment of 28.5°C was also previously reported in wheat, resulting in increased mutation efficiencies as compared to a control temperature of 25.5°C (Milner et al 2020). Heat-treated embryos were exposed to 28.5°C for the entirety of the callus selection phase, totaling 40 days, while the controls were exposed to 28.5°C for 12 days and subsequently grown at 25.5°C for the remaining 28 days of the callus phase. We included 34°C as a treatment in our experiment because it is the temperature at which harvested seed is treated pre-germination. It is the highest temperature that minimally affects tissue morphology and

341 survival, allowing plant cells to regenerate full M_0 plantlets (Table 2) while the Cas9 protein is able
342 to function at a temperature more closely aligned with its bacterial origin allowing for higher protein
343 activity. In this study, we found that regardless of bombardment parameters, a 34°C heat
344 treatment has the most drastic positive effect on mutation efficiency up to 3.68-fold higher than
345 any other temperature (Table 3). Heat treatment of 34°C for both rupture pressures, 650 psi and
346 1100 psi with a particle size of 0.6 µm the mutation frequency at the transgenic event levels were
347 17.2% and 36.8% respectively. All other heat treatments for the same bombardment parameters
348 were comparable. For the 650 psi and 1100 psi rupture pressure, mutation efficiencies measured
349 6.1% and 10.0% for the 26°C treatment, 12.0% and 18.2% for the 30°C temperature and finally
350 11.8% and 12.5% for the 37°C temperature, respectively. There was a trend of having higher
351 mutation efficiencies at 1100 psi than 650 psi (Table 3). As a result of this data, we can conclude
352 that 34°C is the optimal temperature at which both the plant and overexpressed Cas9/gRNA can
353 operate to achieve the highest mutation efficiency. The longer incubation at 34°C still remains to
354 be further evaluated for tissue culture response and mutation efficiency.
355 Through the use of heat treatments, we were able to obtain a variety of M_0 mutant
356 genotypes within single genomes as well as across multiple genomes. In the M_0 generation,
357 75.0% (18/24) of the mutants produced were single genome mutations, 12.5% (3/24) were two
358 genome mutations and the remaining 12.5% (3/24) were triple mutants (Table 4). Of the three
359 triple-mutants, PK3A, PK6A and PC14A, the first two events contain biallelic mutations across all
360 three genomes resulting in the PDS knockout albino phenotype; all mutations were out of frame.
361 (Fig. 5; Tables 4 and 5). In order to obtain the albino PDS phenotype, biallelic mutations in all
362 three genomes or mutations on all 6 loci are required (Table 5). To our knowledge, this is the first
363 report of generating wheat plants with the albino PDS phenotype at the M_0 level. Previous studies
364 have achieved M_0 triple-mutant knockouts but were not able to achieve a phenotype in the M_0
365 generation (Wang et al. 2014). Abe et al. (2019) also generated triple-mutation knockouts on the
366 *TaQsd1* gene for inhibition of preharvest sprouting in the M_1 generation by crossing a M_0 triple-
367 mutant consisting of two biallelic mutations and one monoallelic mutation to WT fielder and
368 segregating in future generations. Both of our M_0 biallelic triple-mutants were derived from the
369 34°C heat treatment, supporting the hypothesis that heat treating transformed material increases
370 the activity of the Cas9 protein/gRNA resulting in higher mutation efficiencies. In order to
371 demonstrate the albino phenotype in M_1 progeny plants derived from a PDS gene-edited event,
372 we used event PC14A having heterozygous monoallelic mutations on both A and D genomes and
373 a heterozygous biallelic mutation on the B genome (Table 4). M_1 progeny from 2 out of 28
374 germinated seedlings of PC14A demonstrated the albino phenotype and showed a 15:1

segregation pattern (Fig. 6; Table 6). Genotyping analysis of these 2 albino phenotype events resulted in homozygous biallelic mutations on both A and D genomes and a heterozygous biallelic mutation on B genome (Table 6) confirming that the albino phenotype requires biallelic mutations across all three genomes. In addition, M_2 progeny from all 3 M_1 lines tested, PC14A-13, PC14A-24 and PC14A-27 with homozygous biallelic mutations on 2 genomes and a heterozygous monoallelic mutation on the remaining 1 genome (Table 6), showed a 3:1 segregation ratio of green and albino PDS phenotype (Table 7). All M_2 progeny plants showing albino PDS phenotype had homozygous biallelic mutations on all 3 genomes (Table 7).

In conclusion, we improved transformation efficiencies in Fielder across all tested delivery pressures using 0.6 μm gold particles for bombardment. We successfully demonstrated an increase in mutation efficiency using heat treatments post bombardment. A heat treatment of 34°C for 24 hours post bombardment resulted in the highest mutation frequency and derived an albino PDS phenotype in the M_0 generation of 2 mutant events, which requires biallelic mutations in all three genomes of hexaploid wheat. Utilizing optimal transformation parameters and a 34°C heat treatment greatly increases mutation efficiency in hexaploid wheat and can help advance research efforts in wheat genomics. The results in this study can be applied to optimize the transformation frequency and improve mutation efficiency in other crop species.

Table 1. Stable transformation frequency of wheat cv. Fielder at T_0 plant level using different bombardment parameters

Stable transformation frequencies for the three combinations of gold particle size and bombardment rupture pressure. a) Column 1 shows the transformation frequencies for 0.4 µm gold particles at rupture pressures of 650 psi, 900 psi and 1100 psi as well as the total transformation frequency of 0.4 µm as a whole. b) Column 2 shows the transformation frequencies for 0.6 µm gold particles at rupture pressures of 650 psi, 900 psi and 1100 psi as well as the total transformation frequency of 0.6 µm as a whole. c) Column 3 shows the transformation frequencies for 1.0 µm gold particles at rupture pressures of 650 psi, 900 psi and 1100 psi as well as the total transformation frequency of 1.0 µm as a whole.

	DsRED + HPT																	
	0.4 um[a]						0.6 um[b]						1.0 um[c]					
	650 psi		900 psi		1100 psi		650 psi		900 psi		1100 psi		650 psi		900 psi		1100 psi	
Transformation frequency*	*12.9%*	13/101	*11.8%*	13/110	*7.7%*	9/117	*24.3%*	25/103	*21.6%*	24/111	*21.9%*	25/114	*7.9%*	10/126	*9.0%*	10/111	*10.3%*	12/117
	10.7% (35/328)						**22.6% (74/328)**						**9.0% (32/354)**					

*Transformation frequency: (# events/# IEs bombarded) x 100%

Table 2. Effect of temperature treatment on callus tissue quality and growth in wheat

Tissue culture heat treatment data. Table expressing the results of a 1-day osmoticum treatment followed by a 1-day temperature treatment of 10 embryos each and the final weight of the tissue after 35 days of callus induction expressed in grams.

Temperature Treatment	Tissue Quality	Tissue Growth (g)
26°C	+++++	1.66
30°C	++++	1.59
34°C	+++(+)	1.70
37°C	+	1.37

Table 3. Mutation efficiency with four different temperature and two bombardment rupture pressure treatments in wheat.

Summary of experimental factors with associated mutation efficiencies and transformation frequencies for each data set. a) Temperature treatment - 1 day temperature treatment at stated temperature, 4 days post bombardment. b) Transformation frequency at T_0 plant level - calculated as the number of transgenic events produced divided by the total number of embryos bombarded. c) Mutation efficiency at transgenic event level - calculated as the total number of mutation events divided by the total number of transgenic events. d) Mutation efficiency at donor embryo level - calculated as the total number of mutation events divided by the total number of embryos bombarded.

Temperature treatments[a]	Bombardment parameters	# embryos bombarded	# transgenic events	Transformation frequency at T_0 plant level[b]	# mutation events	Mutation efficiency at transgenic event level[c]	Mutation efficiency at donor embryo level[d]
26°C	0.6 µm 650 psi	219	33	15.1%	2	6.1%	0.9%
	0.6 µm 1100 psi	130	20	15.4%	2	10.0%	1.5%
	Subtotal	**349**	**53**	**15.2%**	**4**	**7.5%**	**1.1%**
30°C	0.6 µm 650 psi	220	25	11.4%	3	12.0%	1.4%
	0.6 µm 1100 psi	131	11	8.4%	2	18.2%	1.5%
	Subtotal	**351**	**36**	**10.3%**	**5**	**13.9%**	**1.4%**
34°C	0.6 µm 650 psi	221	29	13.1%	5	17.2%	2.3%
	0.6 µm 1100 psi	131	19	14.5%	7	36.8%	5.3%
	Subtotal	**352**	**48**	**13.6%**	**12**	**25.0%**	**3.4%**
37°C	0.6 µm 650 psi	223	17	7.6%	2	11.8%	0.9%
	0.6 µm 1100 psi	131	8	6.1%	1	12.5%	0.8%
	Subtotal	**354**	**25**	**7.1%**	**3**	**12.0%**	**0.8%**

Table 4. Mutation patterns and phenotypes in genome-edited wheat events generated by four different temperature and two bombardment rupture pressure treatments

Temperature treatments	Bombardment parameters	Event name	Mutation			Phenotype
			A genome	B genome	D genome	
26°C	0.6 μm 650 psi	PI9A	WT	WT	[a]1-bp in	Green
		PI22A	WT	[a]1-bp del	WT	Green
	0.6 μm 1100 psi	PA1C	WT	Mutation	WT	Green
		PA11A	[a]1-bp del	WT	WT	Green
30°C	0.6 μm 650 psi	PJ3A	WT	[c]5-bp del	WT	Green
		PJ7B	WT	WT	[a]1-bp in	Green
		PJ33A	WT	[a]1-bp in (1-bp rep)	WT	Green
	0.6 μm 1100 psi	PB9C	WT	WT	[a]1-bp in	Green
		PB10A	WT	WT	mutation	Green
34°C	0.6 μm 650 psi	PK3A	[c]2-bp del	[c]19-bp del	[b]4-/4-bp del	Albino
		PK5A	[a]17-bp del	[b]3-/8-bp del	WT	Green
		PK6A	[b]1-bp in/13-bp del	[b]5-bp del (1-bp rep) /5-bp del	[b]1-bp in/4-bp del	Albino
		PK7A	WT	WT	[c]3-bp del	Green
		PK20B	Mutation	WT	WT	Green
	0.6 μm 1100 psi	PC4C	WT	WT	[a]1-bp in (1-bp rep)	Green
		PC5A	WT	[a]13-bp del	[b]2-bp in/1-bp del	Green
		PC6A	[a]5-bp del	Mutation	WT	Green
		PC6B	WT	Mutation	WT	Green
		PC8C	WT	[a]2-bp in	WT	Green
		PC11A	WT	WT	[a]1-bp in	Green
		PC14A	[a]8-bp del	[b]1-/4-bp del	[a]1-bp in	Green
37°C	0.6 μm 650 psi	PL1B	WT	[b]3-bp del/8-bp del	WT	Green
		PL6A	WT	[a]3-bp del	WT	Green
	0.6 μm 1100 psi	PD5A	WT	[a]1-bp in	WT	Green

WT: wild-type

[a]heterozygous monoallelic

[b]heterozygous biallelic

[c]homozygous biallelic

Table 5. Molecular analysis of M_0 PDS knockout plantlets showing albino phenotype

Molecular analysis of 2 albino phenotype PDS mutation events indicating biallelic mutations across all genomes and sequence.

Albino PDS Event	Genome	Mutation type	Sequence	Biallelic mutation on all 3 genomes
PK3A	A	homozygous biallelic	ATGACCACCTTCTTT- -AGCAGGTATGTC	2-bp deletion
	B	homozygous biallelic	AT- - - - - - - - - - - - - - - - - - -GGTATGTC	19-bp deletion
	D	heterozygous biallelic	ATGACCACCTTCT- - - -AGCAGGTATGTC	4-bp deletion
			ATGACCACCTTCTTTT - - - - AGGTATGTC	4-bp deletion
PK6A	A	heterozygous biallelic	ATGACCACCTTCTTTTCAAGCAGGTATGTC	1-bp insertion
			ATGACCAC- - - - - - - - - - - - -GGTATGTC	13-bp deletion
	B	heterozygous biallelic	ATGACCACCTTT- - - - - AGCAGGTATGTC	5-bp deletion/1 bp (C->T) replacement
			ATGACCACCTTC- - - - -AGCAGGTATGTC	5-bp deletion
	D	heterozygous biallelic	ATGACCACCTTCTTTTCGAGCAGGTATGTC	1-bp insertion
			ATGACCACCTTC- - - -AGCAGGTATGTC	4-bp deletion

Table 6. Phenotype and molecular analysis of M_1 progeny plants derived from of PC14A

PC14A is an M_0 event with heterozygous monoallelic mutations in the A and D genomes and a heterozygous biallelic mutations in the B genome.

M_1 progeny	A genome	B genome	D genome	Phenotype
PC14A-1	WT	homo (1 bp del)	WT	green
PC14A-2	WT	hetero*	hetero	green
PC14A-3	homo (8 bp del)	homo (4 bp del)	hetero	green
PC14A-4	homo (8 bp del)	hetero*	homo (1b in)	albino
PC14A-5	hetero	homo (1 bp del)	hetero	green
PC14A-6	hetero	homo (1 bp del)	WT	green
PC14A-7	hetero	hetero*	hetero	green
PC14A-8	homo (8 bp del)	hetero*	homo (1b in)	albino
PC14A-9	homo (8 bp del)	hetero*	hetero	green
PC14A-10	hetero	homo (1 bp del)	hetero	green
PC14A-11	WT	hetero*	hetero	green
PC14A-12	hetero	homo (4 bp del)	hetero	green
PC14A-13	hetero	homo (1 bp del)	homo (1b in)	green
PC14A-14	hetero	hetero*	WT	green
PC14A-15	??	homo (1 bp del)	hetero	green
PC14A-16	hetero	hetero*	hetero	green
PC14A-17	homo (8 bp del)	homo (4 bp del)	WT	green
PC14A-18	WT	hetero*	hetero	green
PC14A-19	homo (8 bp del)	hetero*	hetero	green
PC14A-20	hetero	hetero*	hetero	green
PC14A-21	WT	homo (1 bp del)	hetero	green
PC14A-22	hetero	hetero*	homo (1b in)	green
PC14A-23	hetero	hetero*	hetero	green
PC14A-24	hetero	homo (4 bp del)	homo (1b in)	green
PC14A-25	WT	hetero*	WT	green
PC14A-26	WT	homo (4 bp del)	homo (1b in)	green
PC14A-27	homo (8 bp del)	homo (1 bp del)	hetero	green
PC14A-28	hetero	homo (4 bp del)	hetero	green

*hetero biallelic

Table 7. Phenotype and molecular analysis of M_2 progeny plants derived from of three M_1 PC14A lines. PC14A-13 and PC14A-24 are M_1 progeny lines derived from PC14A. Both lines have homozygous biallelic mutations on both B and D genomes and a heterozygous monoallelic mutation on the A genome while PC14A-27 is M_1 progeny line with homozygous biallelic mutations on both A and B genomes and a heterozygous monoallelic mutation on the D genome (A) Plant phenotype of M_2 progeny plants derived from three M_1 PC14A lines. (B) Genotype of M_2 PDS albino plants derived from three M_1 PC14A lines.

(A)

M1 progeny	Segregation ratio of M_2 progeny plants (green: albino)
PC14A-13	13: 2*
PC14A-24	11: 4*
PC14A-27	11: 5*

*Analyses using a χ^2-test indicate that the segregation ratios of progeny plants for GFP were not significantly different from 3:1 (at $\alpha = 0.05$)

(B)

M_1 progeny	A genome	B genome	D genome	Phenotype
PC14A-13-1	homo (8 bp del)	homo (1 bp del)	homo (1b in)	albino
PC14A-13-2	homo (8 bp del)	homo (1 bp del)	homo (1b in)	albino
PC14A-24-1	homo (8 bp del)	homo (4 bp del)	homo (1b in)	albino
PC14A-24-2	homo (8 bp del)	homo (4 bp del)	homo (1b in)	albino
PC14A-24-3	homo (8 bp del)	homo (4 bp del)	homo (1b in)	albino
PC14A-24-4	homo (8 bp del)	homo (4 bp del)	homo (1b in)	albino
PC14A-27-1	homo (8 bp del)	homo (1 bp del)	homo (1b in)	albino
PC14A-27-2	homo (8 bp del)	homo (1 bp del)	homo (1b in)	albino
PC14A-27-3	homo (8 bp del)	homo (1 bp del)	homo (1b in)	albino
PC14A-27-4	homo (8 bp del)	homo (1 bp del)	homo (1b in)	albino
PC14A-27-5	homo (8 bp del)	homo (1 bp del)	homo (1b in)	albino

Figure Legends

Figure 1. Schematic diagrams of three transformation vectors used for wheat transformation and gene editing. (A) pAct1IHPT-4 is a 5,870-bp plasmid containing hygromycin phosphotransferase (HPT) driven by the OsAct1 promoter and its intron. (B) pAct1IDsRED is a 5,139-bp plasmid containing DsRED driven by the OsAct1 promoter and its intron. (C) pRGE-PDS-PS2 is a 10,122-bp plasmid containing 2 gene cassettes where gRNA is driven by the Tau6 promoter and Cas9 driven by OsUbi10 promoter.

Figure 2. Stable wheat transformation via biolistics. (B) Harvest immature wheat spikes 10-14 days post-anthesis. (B) Isolate immature embryos sized 1.7-2.2 mm and place on osmoticum medium for 4 hours. (C) Shoot gold particles with gene gun and desired gold particle size and rupture disc pressure (D) Plant tissue is subjected to three rounds of callus induction media containing selection, subculturing every 3 weeks (E) Larger callus pieces derived from a single immature embryos are broken up and placed on regeneration medium for shoot formation (F)

Plantlets that are at least 1 cm in height are transferred to rooting medium in Phytatrays and grown to size until they can be transferred to soil.

Figure 3. DsRED expression in different tissue types in transgenic wheat. (A) Transient DsRED expression and brightfield of an immature wheat embryo 3 days post bombardment. (B) The formation of a DsRED sector growing 6-8 weeks post bombardment compared with brightfield image of the same sector. (C) A stable transformation showing DsRED expression in leaf tissue in comparison to a wild-type control. (D) A stably transformed DsRED plantlet 10-12 weeks post bombardment under fluorescence and brightfield.

Figure 4. Volume (Weight) and surface area of different gold particle sizes. Different gold particles are capable of holding different quantities of DNA. (A) The diameter of a sphere directly affects the number of gold particles by weight. As diameter increases, the number of gold particles in a fixed weight decreases. The smaller the gold particle the more particles will be available to be coated in DNA for each bombardment prep. (B) Larger diameter directly affects surface area of each particle. The larger the diameter, the greater the surface area. The difference in diameter between 0.4 µm to 1.0 µm results in a 6.25-fold increase in surface area. This means that larger particles are capable of holding a greater amount of DNA.

Figure 5. Triple biallelic knockout mutants showing albino phenotype. Photos depicting albino PDS triple biallelic mutants in plates as well as in Phytatrays. Both albino events #1 and #2 produced as a result of the 34°C 1-day heat treatment, shown in plate and Phytatray.

Figure 6. Phenotype of M_1 progeny plants derived from event PC14A with monoallelic and biallelic mutations in the 3 different genomes. M_1 progeny segregation from PC14A which contained two monoallelic mutations and 1 biallelic mutation. Photo of 2 albino M_1 progeny of the 28 total plantlets (red arrows).

Supplementary Information

Table S1. Primer sets used for selection of transgenic plants and for mutation in genome-edited plants

Table S2. Microcarrier size effect on DsRED co-expression efficiency

Figure S1. Microcarrier size effect on transient DsRED expression and genome editing efficiency (A) Photos were taken for transient DsRED expression 3 days post bombardment. (B) Sanger sequencing was performed to detect mutations in all 3 genomes of each transgenic event.

Acknowledgements

We are grateful to Dr. Juliana Matos and Dominick Tucker for, the pAct1IDsRED plasmid and plant care in the growth chambers and greenhouse, respectively.

Funding

This work was supported by the IGI of the University of California at Berkeley.

Compliance with ethical standards

Conflict of interest The authors declare that they have no conflict of interest.

602 **References**

603

604 Abe F, Haque E, Hisano H, Tanaka T, Kamiya Y, Mikami M, Kawaura K, Endo M, Onishi K,
605 Hayashi T, Sato K (2019) Genome-edited triple-recessive mutation alters seed dormancy in
606 wheat. Cell Rep 28: 1362-1369. https://doi.org/10.1016/j.celrep.2019.06.090

607

608 Bartley GE, Scolnik PA (1995) Plant carotenoids: pigments for photoprotection, visual attraction,
609 and human health. Plant Cell 7: 1027–38. https://doi.org/10.1105/tpc.7.7.1027

610

611 Bortesi L, Fischer R (2015) The CRISPR/Cas9 system for plant genome editing and beyond.
612 Biotechnol Adv 33: 41–52. https://doi.org/10.1016/j.biotechadv.2014.12.006

613

614 Cho M-J, Jiang W, Lemaux PG (1998) Transformation of recalcitrant barley cultivars through
615 improvement of regenerability and decreased albinism. Plant Sci 138: 229–244.
616 https://doi.org/10.1016/ S0168-9452(98)00162-9

617

618 Cho M-J, Ha CD, Lemaux PG (2000) Production of transgenic tall fescue and red fescue plants
619 by particle bombardment of mature seed-derived highly regenerative tissues. Plant Cell Rep 19:
620 1084-1089. https://doi.org/10.1007/s002990000238

621

622 Cho M-J, Banh J, Yu M, Kwan J, Jones TJ (2015) Improvement of *Agrobacterium*-mediated
623 transformation frequency in multiple modern elite commercial maize (*Zea mays* L.) inbreds by
624 media modifications. Plant Cell Tiss Organ Cult 121: 519-529. https://doi.org/10.1007/s11240-
625 015-0721-7

626

627 Choi HW, Lemaux PG, Cho M-J (2002) Use of fluorescence in situ hybridization for gross mapping
628 of transgenes and screening for homozygous plants in transgenic barley (*Hordeum vulgare* L.).
629 Theor Appl Genet 106: 92-100. https://doi.org: 10.1007/s00122-002-0997-y

630

631 Dai S, Zhang P, Marmey P, Zhang S, Tian W, Chen S, Beachy R, Fauquet C (2001) Comparative
632 analysis of transgenic plants obtained by *Agrobacterium*-mediated transformation and particle
633 bombardment. Mol Breed 7:25–33. https://doi.org/10.1023/A:1009687511633

634

635 Doudna JA, Charpentier E (2014) Genome editing. The new frontier of genome engineering with
636 CRISPR-Cas9. Science 346: 1258096. https://doi.org/10.1126/science.1258096
637
638 Feng Z, Zhang B, Ding W et al. (2013) Efficient genome editing in plants using a CRISPR/Cas
639 system. Cell Res 23: 1229–1232. https://doi.org/10.1038/cr.2013.114
640
641 Finer JJ, Finer KR, Ponappa T (2000) Particle bombardment mediated transformation. In:
642 Hammond J, McGarvey P, Yusibov V (eds) Plant Biotechnology. Current Topics in Microbiology
643 and Immunology, vol 240. Pages 59-80, Springer, Berlin, Heidelberg. https://doi.org/10.1007/978-
644 3-642-60234-4_3
645
646 Grützner R, Martin P, Hom C, Mortensen S, Cram EJ, Lee-Parsons C, Stuttmann J, Marillonnet
647 S (2021) High-efficiency genome editing in plants mediated by a Cas9 gene containing multiple
648 introns. Plant Communications, Volume 2, Issue 2, 100135, ISSN 2590-3462.
649 https://doi.org/10.1016/j.xplc.2020.100135
650
651 Hart, G. (1983) Hexaploid Wheat (*Triticum aestivum* L. em Thell). Developments in plant genetics
652 and breeding, Elsevier, Volume 1, Part B, Pages 35-56, ISSN 0168-7972.
653 https://doi.org/10.1016/B978-0-444-42227-9.50006-8
654
655 Hooghvorst I, López-Cristoffanini C, Nogués S (2019) Efficient knockout of phytoene desaturase
656 gene using CRISPR/Cas9 in melon. Sci Rep 9: 17077. https://doi.org/10.1038/s41598-019-
657 53710-4
658
659 Howells RM, Craze M, Bowden S, Wallington EJ (2018) Efficient generation of stable, heritable
660 gene edits in wheat using CRISPR/Cas9. BMC Plant Biol 18: 215.
661 https://doi.org/10.1186/s12870-018-1433-z
662
663 Hu T, Metz S, Chay C *et al.* (2003) *Agrobacterium*-mediated large-scale transformation of wheat
664 (*Triticum aestivum* L.) using glyphosate selection. Plant Cell Rep 21: 1010–1019.
665 https://doi.org/10.1007/s00299-003-0617-6
666
667 Jones J, Zhang E, Tucker D, Daniel R, Gomez M, Dahlbeck D, Garcia C, Marelli J-P, Livingstone
668 D, Schnell R, Staskawicz B, Cho M-J (2022) Screening of cultivars for tissue culture response

669 and establishment of genetic transformation in a high-yielding and disease-resistant cultivar of
670 *Theobroma cacao*. In Vitro Cell Dev Biol-Plant 58: 133-145. https://doi.org/10.1007/s11627-021-
671 10205-0
672
673 Klein TM, Fromm M, Weissinger A, Tomes D, Schaff S, Sletten M & Sanford JC (1988) Transfer
674 of foreign genes into intact maize cells with high-velocity microprojectiles. Proc Natl Acad Sci 85:
675 4305-4309. https://doi.org/10.1073/pnas.85.12.4305
676
677 LeBlanc C, Zhang F, Mendez J, Lozano Y, Chatpar K, Irish VF, Jacob Y (2018) Increased
678 efficiency of targeted mutagenesis by CRISPR/Cas9 in plants using heat stress. Plant J 93: 377-
679 386. https://doi.org/10.1111/tpj.13782
680
681 Lemaux PG, Cho M-J, Louwerse J, Williams R, Wan Y (1996) Bombardment-mediated
682 transformation methods for barley. Bio-Rad US/EG Bulletin 2007 p1-6.
683
684 Liu H, Wang K, Jia Z, Gong Q, Lin Z, Du L, Pei X, Ye X (2019) Efficient induction of haploid plants
685 in wheat by editing of TaMTL using an optimized *Agrobacterium*-mediated CRISPR system. J Exp
686 Bot 71, 1337–1349. https://doi.org/10.1093/jxb/erz529
687
688 Malzahn AA, Tang X, Lee K, Ren Q, Sretenovic S, Zhang Y, Chen H, Kang M, Bao Y, Zheng X
689 et al. (2019) Application of CRISPR-Cas12a temperature sensitivity for improved genome editing
690 in rice, maize, and *Arabidopsis*. BMC Biol 17: 9. https://doi.org/10.1186/s12915-019-0629-5
691
692 Milner MJ, Craze M, Hope MS, Wallington EJ (2020) Turning up the temperature on CRISPR:
693 Increased temperature can improve the editing efficiency of wheat using CRISPR/Cas9. Front
694 Plant Sci, 11. https://doi.org/10.3389/fpls.2020.583374
695
696 Murray MG, Thompson WF (1980) Rapid isolation of high molecular weight plant DNA. Nucleic
697 Acids Res 8: 4321–4325. https://doi.org/10.1093/nar/8.19.4321
698
699 Naim F, Dugdale B, Kleidon J, Brinin A, Shand K, Waterhouse P, Dale J (2018) Gene editing the
700 phytoene desaturase alleles of Cavendish banana using CRISPR/Cas9. Transgenic Res 27: 451–
701 460. https://doi.org/10.1007/s11248-018-0083-0
702

703 Odipio J, Alicai T, Ingelbrecht I, Nusinow DA, Bart R and Taylor NJ (2017) Efficient CRISPR/Cas9
704 genome editing of phytoene desaturase in cassava. Front Plant Sci 8: 1780.
705 https://doi.org/10.3389/fpls.2017.01780
706
707 Panos C, Cohen B (1964) Growth rates of *Streptococcus pyogenes* and derived L form at various
708 temperatures. J Bacteriol 87: 1242–1243. https://doi.org/10.1128/jb.87.5.1242-1243.1964
709
710 Poddar S, Tanaka J, Cate JHD, Staskawicz B, Cho M-J (2020) Efficient isolation of protoplasts
711 from rice calli with pause points and its application in transient gene expression and genome
712 editing assays. Plant Methods 16: 151 https://doi.org/10.1186/s13007-020-00692-4
713
714 Qin G, Gu H, Ma L, Peng Y, Deng XW, Chen Z, Qu L-J (2007). Disruption of phytoene desaturase
715 gene results in albino and dwarf phenotypes in *Arabidopsis* by impairing chlorophyll, carotenoid,
716 and gibberellin biosynthesis. Cell Res 17: 471–482. https://doi.org/10.1038/cr.2007.40
717
718 Smith RH, Hood EH (1995) *Agrobacterium tumefaciens* transformation of monocotyledons. Crop
719 Sci 35: 301–309. https://doi.org/10.2135/cropsci1995.0011183X003500020001x
720
721 Wang Y, Cheng X, Shan Q, Zhang Y, Liu J, Gao C (2014) Simultaneous editing of three
722 homoeoalleles in hexaploid bread wheat confers heritable resistance to powdery mildew. Nat
723 Biotechnol 32: 947–951. https://doi.org/10.1038/nbt.2969
724
725 Vain P, Keen N, Murillo J, Rathus C, Nemes C, Finer JJ (1993) Development of the particle inflow
726 gun. Plant Cell Tiss Organ Cult 33: 237-246. https://doi.org/10.1007/BF02319007
727
728 Xiang G, Zhang X, An C, Cheng C, Wang H (2017) Temperature effect on CRISPR-Cas9
729 mediated genome editing. J Genet Genomics, 44: 199–205.
730 https://doi.org/10.1016/j.jgg.2017.03.004.
731
732 Zhang H, Zhang J, Wei P, Zhang B, Gou F, Feng Z, Mao Y, Yang L, Zhang H, Xu N, Zhu J-K
733 (2014) The CRISPR/Cas9 system produces specific and homozygous targeted gene editing in
734 rice in one generation. Plant Biotechnol J 12: 797–807. https://doi.org/10.1111/pbi.12200
735

736 Zhang Z, Hua L, Gupta A, Tricoli D, Edwards K J, Yang B, Li W (2019). Development of an
737 *Agrobacterium*-delivered CRISPR/Cas9 system for wheat genome editing. Plant Biotechnol J 17:
738 1623–1635. https://doi.org/10.1111/pbi.13088
739

(A) pAct1IHPT-4

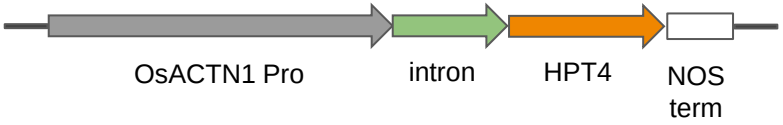

(B) pAct1IDsRED

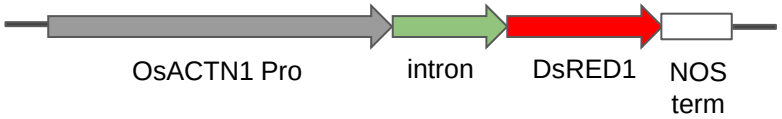

(C) pRGE-PDS-PS2

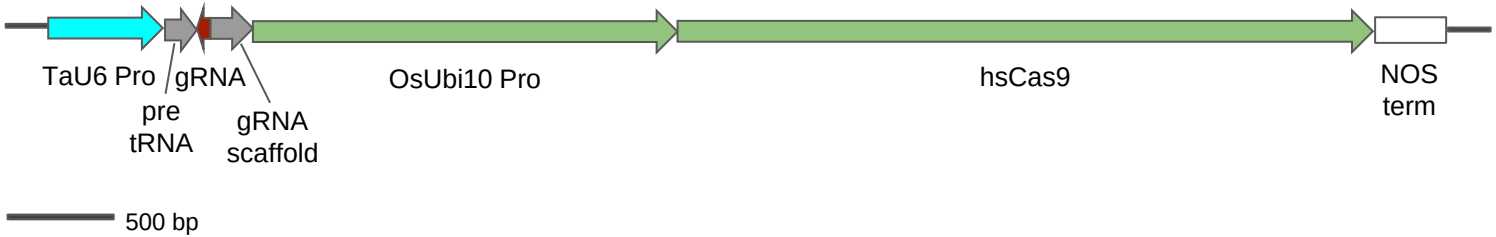

Figure 1.

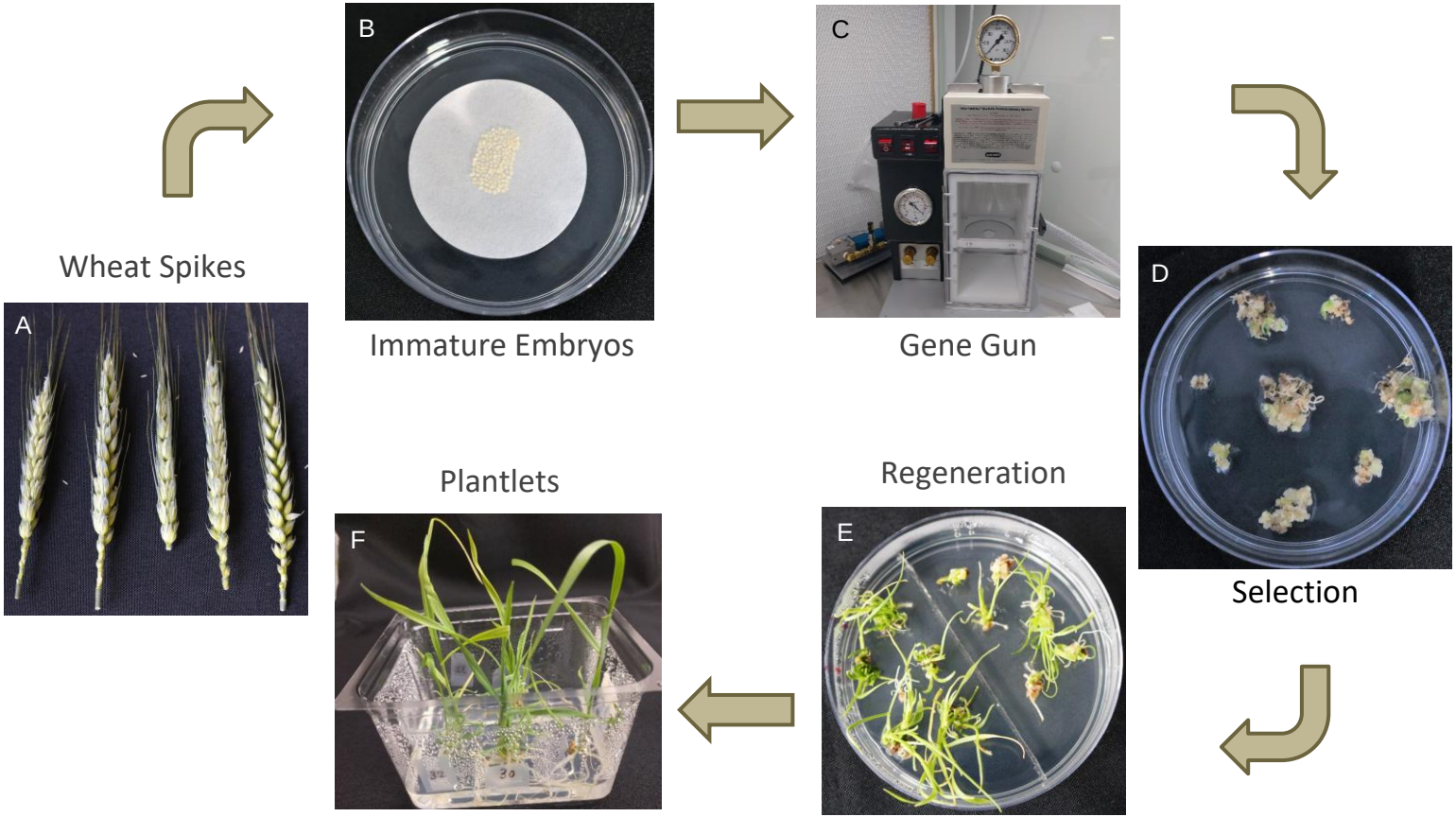
Wheat Spikes
A
B
Immature Embryos
C
Gene Gun
D
Selection
Regeneration
E
Plantlets
F

Figure 2.

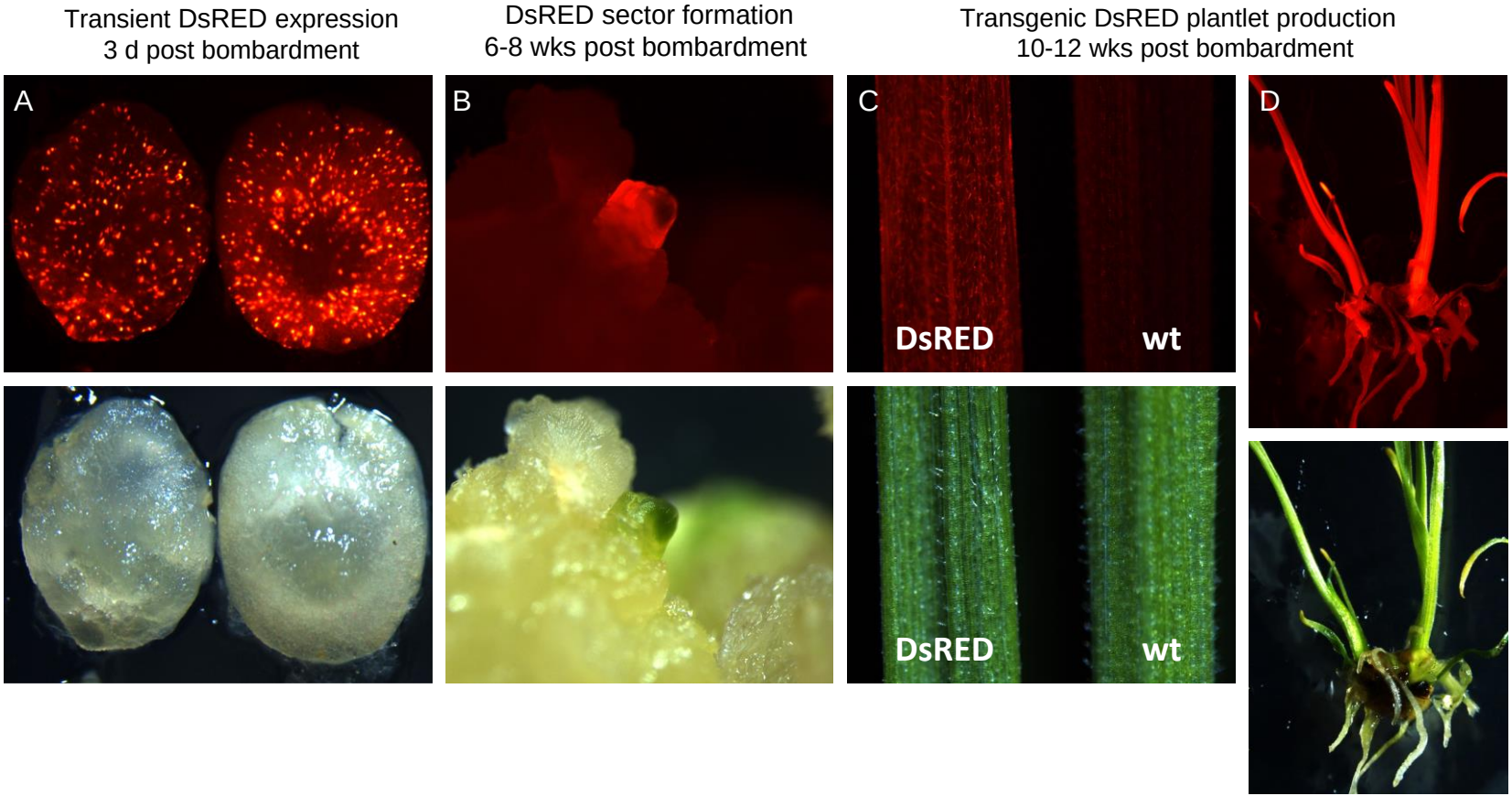
Transient DsRED expression
3 d post bombardment
DsRED sector formation
6-8 wks post bombardment
Transgenic DsRED plantlet production
10-12 wks post bombardment
A
B
C
D
DsRED
wt
DsRED
wt

Figure 3.

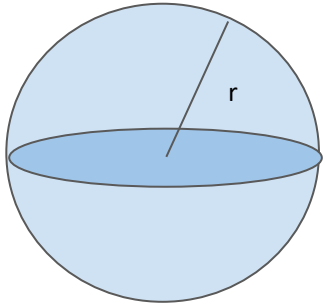

(A) Larger diameter microcarriers confer a smaller # of microcarriers per weight (wt)

Volume = $(4/3)\pi r^3$

Microcarrier Diameter	0.4 µm	0.6 µm	1.0 µm
Volume	0.27 μm^3	0.90 μm^3	4.17 μm^3
Relative Volume (wt)	0.06	0.22	1
Relative # of microcarriers/wt	16.7	4.5	1

(B) Larger diameter microcarriers confer more surface area of each microcarrier

Surface Area = $4\pi r^2$

Microcarrier Diameter	0.4 µm	0.6 µm	1.0 µm
Surface Area	2.01 μm^2	4.52 μm^2	12.56 μm^2
Relative Surface Area	0.16	0.36	1

Figure 4.

Albino event #1
(PK3A)

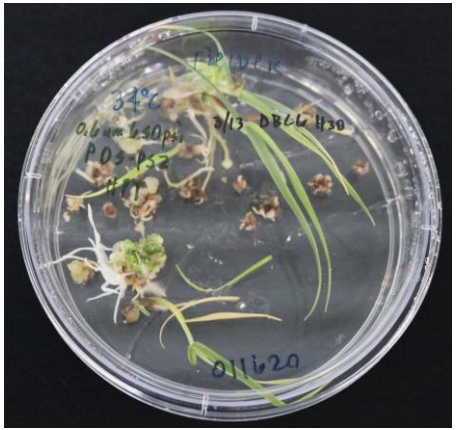

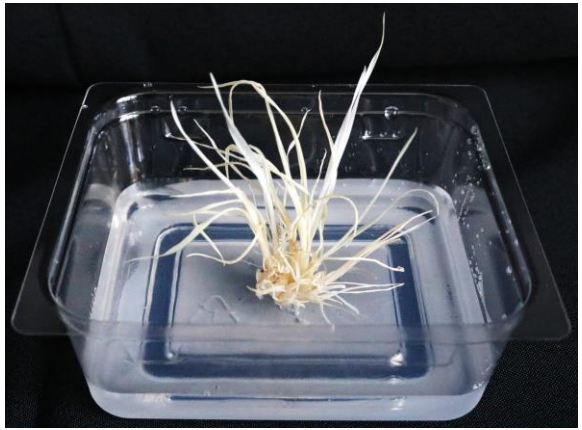

Albino event #2
(PK6A)

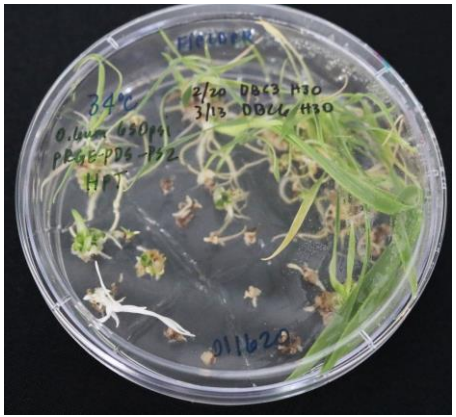

Figure 5.

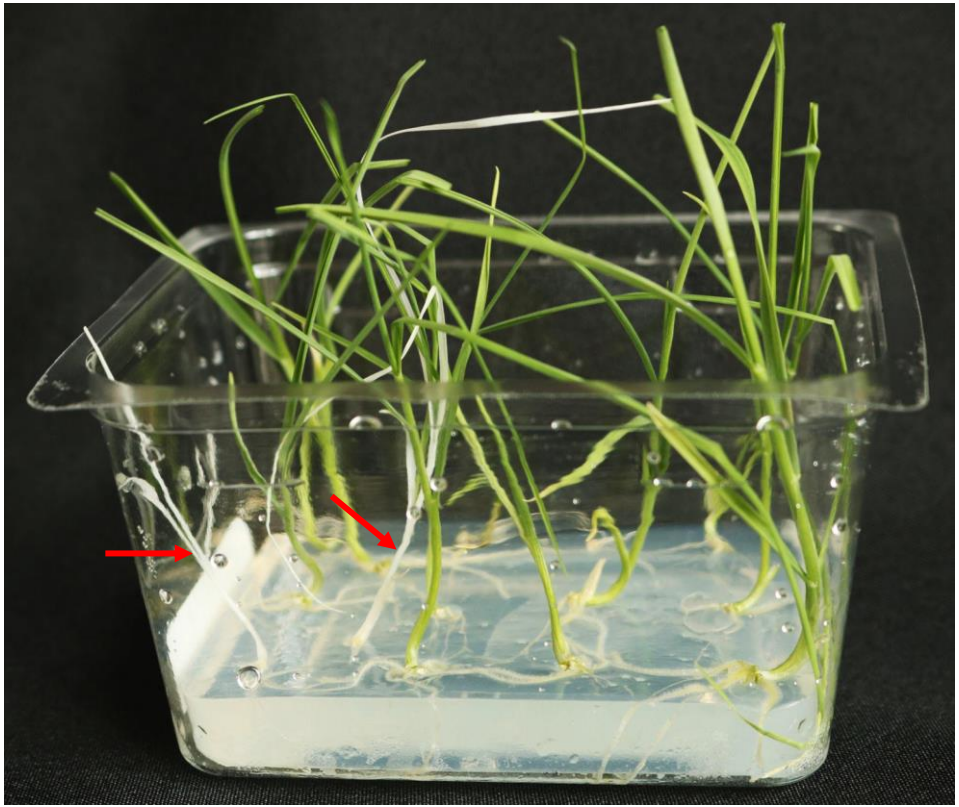

Figure 6.